Available online at www.sciencedirect.com
SCIENCE DIRECT®
International Journal of Heat and Mass Transfer 47 (2004) 2261–2268
International Journal of HEAT and MASS TRANSFER
www.elsevier.com/locate/ijhmt

Ultrafast investigation of electron dynamics in multi-layer metals

Wael M.G. Ibrahim [a,*], Hani E. Elsayed-Ali [a], Carl E. Bonner Jr. [b], Michelle Shinn [c]

[a] Department of Electrical and Computer Engineering and the Applied Research Center, Old Dominion University, Norfolk, VA 23529 USA
[b] Center for Material Research, Norfolk state University, Norfolk, VA 23504 USA
[c] Thomas Jefferson National Accelerator Facility, Newport News, VA 23606 USA

Received 23 March 2003; received in revised form 15 November 2003

Abstract

Ultrafast time-resolved pump–probe studies of energy relaxation and transport in polycrystalline single and multi-layer metal films are presented. The dependence of the surface electron temperature on the film structure was investigated. Vanadium was studied as possible padding layer for increasing the laser damage threshold of metal mirrors. The results, for 300 K $< T_e <$ 700 K, where T_e is the effective electron temperature, show a reduction of the thermoreflectivity signal, ΔR_{max} for the multi-layer structure as compared to the single layer film. This reduction signifies a drop in the surface electron temperature that is in agreement with previous work. Damage experiments, in the high fluence regime, where the thermomodulation data can no longer be related to the effective electron temperature, show that the padding layer does not improve the damage threshold as previously suggested. The experimental results are analyzed within the framework of the two-temperature model (TTM), which agrees well with both thermomodulation and damage results.
Published by Elsevier Ltd.

1. Introduction

In spite of the large number of studies dealing with femtosecond laser interactions with metals and metal multi-layers [1–4], the process of heat transport by the hot electrons in multi-layer metal films remains under study [5]. Optical energy deposition in the surface layer results in electron excitation which in turns relaxes by electron–electron and electron–phonon collisions. The increase in the lattice effective temperature by electron–phonon collisions can cause surface damage. It was suggested that introducing a padding layer under the surface has the potential of increasing the damage threshold [3,4].

A multi-layer configuration of a gold surface padded with chromium was studied as a potential structure that can increase the damage threshold of the gold surface heated by a femtosecond laser. Exploiting the large value of the heat capacity and the electron–phonon coupling coefficient of a chromium padding layer, the chromium would act as a heat sink, absorbing the thermal energy transmitted through the interface and then coupling that energy to the lattice away from the gold surface [3,4]. Results showed a strong dependence of the thermal response of thin metal films on their structures, and suggested the possibility of increasing the resistance of mirror coatings to thermal damage under high power femtosecond laser irradiation.

Further investigations of candidate padding layers, depending on the values of their heat capacity and the electron–phonon coupling coefficient, are warranted. An understanding of heat transport in laser-irradiated multi-layer films and the potential of developing optical films with higher damage threshold motivated the present work. The effect of introducing vanadium, V, padding layer, which has an electron–phonon coupling

* Corresponding author.
E-mail address: wibrahim@ecpi.edu (W.M.G. Ibrahim).

0017-9310/$ - see front matter Published by Elsevier Ltd.
doi:10.1016/j.ijheatmasstransfer.2003.11.029

Nomenclature

$C_e(T_e)$	electron heat capacity ($J\,m^{-3}\,K^{-1}$)
$C_l(T_l)$	lattice heat capacity ($J\,m^{-3}\,K^{-1}$)
d	film thickness (m)
G	e–ph coupling coefficient ($W\,m^{-3}\,K^{-1}$)
H	source term ($W\,m^{-3}$)
J	laser pulse energy ($J\,m^{-2}$)
R	surface reflectivity
t	time (s)
t_p	laser pulse duration (s)
T	transmissivity
T_e	effective electron temperature (K)
T_l	effective lattice temperature (K)
$S(t)$	system response function
x	spatial coordinate (m)

Greek symbols

δ	the radiation penetration depth (m)
δ_b	ballistic range of electrons (m)
γ	constant ($J\,m^{-3}$)
κ	thermal conductivity ($W\,m^{-1}\,K^{-1}$)
κ_o	thermal conductivity under equilibrium conditions ($W\,m^{-1}\,K^{-1}$)
Θ_D	Debye temperature (K)
τ	electron relaxation time (s)
τ_R	electron–electron equilibration time (s)

coefficient one order of magnitude higher than chromium, is investigated. A comparison of the predicted electron temperature, using the two-temperature model (TTM) with the experimental results is also presented. Damage experiments on the single and multi-layer structures are conducted to test the aforementioned hypothesis.

2. Model

In ultrafast laser heating of metals, a transient non-equilibrium occurs between the effective electron temperature, T_e, and the effective lattice temperature, T_l, due to the small heat capacity of the electrons. For times longer than the electron–electron interaction time, thermalization of the hot electrons occurs. Under these conditions, the treatment of the heating process can be composed of two individual processes: (1) the absorption of photon energy by the electrons and (2) the subsequent equilibration of the electron gas and the lattice through electron–phonon coupling. The overall heating process can then be modeled using TTM, initially proposed by Anisimov et al. as [6]:

$$\begin{aligned} C_e(T_e)\frac{\partial T_e}{\partial t} &= \frac{\partial}{\partial x}\left(\kappa\frac{\partial T_e}{\partial x}\right) - G(T_e - T_l) + H \\ C_l(T_l)\frac{\partial T_l}{\partial t} &= G(T_e - T_l) \end{aligned} \tag{1}$$

Where κ is the thermal conductivity ($W\,m^{-1}\,K^{-1}$), $C_e(T_e)$ is the electron heat capacity ($J\,m^{-3}\,K^{-1}$), $C_l(T_l)$ is the lattice heat capacity ($J\,m^{-3}\,K^{-1}$), T_e is the electron effective temperature (K), T_l is the lattice effective temperature (K), G is the electron–phonon coupling coefficient ($W\,m^{-3}\,K^{-1}$), and H is the source term ($W\,m^{-3}$).

Due to the nonlinear temperature dependence of the electronic heat capacity, $C_e(T_e)$ Eq. (1) was solved numerically using finite element method. The electronic heat capacity can be approximated by a linear function of the electron temperature $C_e(T_e) = \gamma T_e$, γ being a constant, as long as T_e is much smaller than the Fermi energy, which is 5.53 eV (64 150 K) for Au [1]. The lattice heat capacity C_l can be assumed to be a constant for temperatures above the Debye temperature Θ_D which is 165 K for Au [7]. The dependence of the thermal conductivity κ on T_e and T_l was expressed as $\kappa = \kappa_o[T_e/T_l]$, which did not affect the dynamics of the solution for low electron temperature excursions [3].

The transient thermomodulation data were compared to the predicted effective electron and lattice temperatures from TTM. The thermomodulation signal is assumed proportional to the effective electron temperature excursion, for relatively small excursions. The boundary conditions used neglect heat losses from the front and back surfaces of the sample. $\frac{\partial T_e}{\partial x}|_{x=0} = \frac{\partial T_e}{\partial x}|_{x=d} = \frac{\partial T_l}{\partial x}|_{x=0} = \frac{\partial T_l}{\partial x}|_{x=d} = 0$. The electron heat flux and temperature at the gold–vanadium interface are continuous: $\kappa\frac{\partial T_e}{\partial x}|_{Au} = \kappa\frac{\partial T_e}{\partial x}|_{V}$, and $T_e|_{Au} = T_e|_{V}$.

The electron and lattice effective temperatures were used as the two variables for which the equations are solved. The initial conditions for the electron and the lattice systems were chosen as $T_e(x, -2t_p) = T_l(x, -2t_p) = 300$ K, where t_p is the laser pulse full-width at half-maximum (FWHM). The physical properties of gold and vanadium, listed in Table 1, were used in the model. The exact value of G for Au used in the model was the value that provided best fit to our data, which was $G = 2.3 \times 10^{16}\ W\,m^{-3}\,K^{-1}$. The source term, H, in the two-temperature model represented a Gaussian pulse specified in the model as:

$$H = 0.94\frac{1-R}{t_p\delta}J \cdot \exp\left[-\frac{x}{\delta} - 2.77\left(\frac{t}{t_p}\right)^2\right] \tag{2}$$

Table 1
Room temperature properties of the metals used in Ref. [4] and present experiments

	Au	V	Cr
Measured 'G' ($\mathrm{W\,m^{-3}\,K}$)[a]	2.8 ± 0.5	523 ± 37	$42 \pm 5 \times 10^{16}$
Melting point (°C)[b]	1063	1900	1875
Density ($\mathrm{g\,cm^{-3}}$)[b]	19.3	6.11	7.19
Thermal conductivity κ_o ($\mathrm{W\,m^{-1}\,K}$)[b]	315	30	94
Electron heat capacity C_e ($\mathrm{J\,m^{-3}\,K^{-1}}$)[b]	2.1	35.24	5.8×10^4
Lattice heat capacity C_l ($\mathrm{J\,m^{-3}\,K^{-1}}$)[b]	2.5	3	3.3×10^6

[a] From data complied in Ref. [1].
[b] Ref. [7].

where R is the reflectivity, δ is the radiation penetration depth (skin depth), and J is the total energy carried by the laser pulse divided by the laser spot size. The present model predictions are in good agreement with those published by Wellerschoff et al. [8]

The TTM has proved to be a good approximation to the thermomodulation experimental results when times considered are longer than that needed to establish an effective electron temperature. However, due to the absence of a ballistic term in the TTM, it tends to underestimate the energy deposition depth [9]. Hohlfeld et al. [9] modified the source term to account for the ballistic electron motion, changing it to

$$H = 0.94\frac{1-R-T}{t_p(\delta+\delta_b)}J\cdot\exp\left[-\frac{x}{(\delta+\delta_b)}-2.77\left(\frac{t}{t_p}\right)^2\right]\cdot\frac{1}{\left(1-\exp\left(-\frac{d}{\delta+\delta_b}\right)\right)} \quad (3)$$

where R is the reflectivity, T is the transmissivity, δ is radiation penetration depth, δ_b is the ballistic range, J is as before the total energy in the laser pulse divided by the laser spot size, and t_p is the FWHM of the laser pulse. In our modeling, we adopted this modification to the source term to account for the ballistic motion of the electrons and hence extending the energy deposition depth. The value of the ballistic range δ_b for Au that provided best agreement with thermomodulation data was found to be 105 nm [8]. Since all films we studied had a thickness less than that, δ_b was taken in our model to be equal to Au thickness in the single layer and the top Au thickness in the multi-layer film.

The TTM assumes an effective electron temperature. To account for the delayed equilibration of the electrons by e–e collisions, we included a response function as described later when comparing the thermomodulation results with the model. The TTM also assumes that the phonon subsystem is at equilibrium with itself. Phonon–phonon equilibration occurs through scattering described by the anharmonic potential. Evaluating the thermalization time of the phonons at 300 K provides an upper limit on that time which is on the order of 10^{-11} s [10]. For weak excitation, where the effective lattice temperature is only perturbed by a small fraction from its initial value, it is reasonable to assume that the small component of nonequilibrium phonons do not affect the electron–phonon relaxation process. This, however, is not the case when large temperature excursions result from femtosecond laser heating in the damage experiments. In this case the lattice temperature is not defined and T_l can only be referred to as an effective temperature. The presence of high density of nonequilibrium phonons could conceivably affect hot electron relaxation and transport. In Au only acoustic phonons can be excited, thus a single-scattering event with an excited electron does not significantly perturb the electron energy. The nonequilibrium phonons could in principle affect the melting dynamics, thus, the damage threshold. However, results obtained by Wellerschoff et al. [8] on femtosecond laser damage of metals such as Au, have shown that the onset of melting as obtained from the TTM defined the damage threshold. Thus, it is reasonable to assume that, for Au, the nonequilibrium phonons do not noticeably affect the melting dynamics.

3. Experimental system

Femtosecond time-resolved thermoreflectivity ($\Delta R/R$) measurements were performed using a collinear pump–probe setup. The laser system used in the thermomodulation studies was a Ti:sapphire oscillator followed by a regenerative amplifier. The input to the experimental setup consisted of ~500 mW pulses at $\lambda = 800$ nm, 250 kHz repetition rate with a FWHM <200 fs. Retroreflecting mirrors mounted on a computer-controlled stage formed the delay line in the pump arm. A half-wave plate is used to make the pump and probe beams orthogonally polarized. White-light continuum generated in a 6-mm sapphire crystal supplied the probe beam. Differential detection was used so as to cancel out the fluctuations of the laser output, leaving only the signal caused by the chopped pump beam. Thus, the lock-in amplifier detects modulation in the received probe intensity that is caused only by the effect of the pump on the sample.

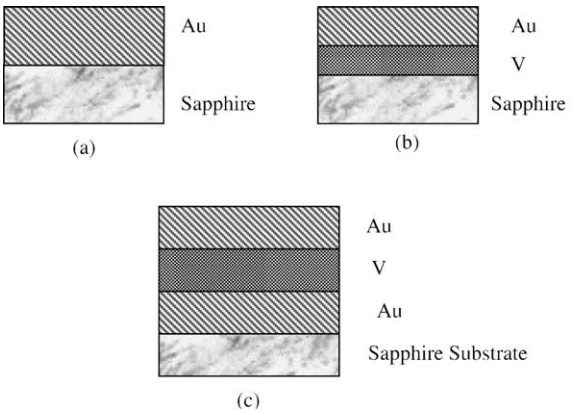

Fig. 1. Schematic diagram of the samples used in the experimental investigations (a) single layer, (b) multi-layer, (c) sandwiched structure.

The laser used in the damage experiments is a commercially available titanium–sapphire laser, with a chirped pulse amplification system pumped by the second harmonic of a Nd:YLF laser at 1 kHz repetition rate. Laser pulses at 800 nm wavelength and 110 fs pulse width were used. A mechanical shutter controlled the exposure time of the sample, i.e., number of laser pulses. All measurements were done in air and at room temperature.

The samples used in the thermomodulation experiments are polycrystalline single and double-layer gold and vanadium thin films deposited on sapphire substrates, Fig. 1(a) and (b). In the damage experiments, single layer gold films, Fig. 1(a), and sandwiched vanadium layer, Fig. 1(c), were used. The thin films were prepared using resistive heating evaporation. The deposition pressure was lower than 10^{-5} Torr and the growth rate around 1 nm s^{-1}.

4. Thermoreflectivity measurements

Femtosecond time-resolved thermoreflectivity ($\Delta R/R$) measurements on polycrystalline single- and multilayer thin films of the same total thickness, as shown in Fig. 1, were conducted. The experimental results are analyzed within the framework of the TTM which assumes that the electron and the lattice subsystems are identified by their respective effective temperatures, T_e and T_l. Numerical solution of Eq. (1) yields the temporal and spatial evolution of these temperatures. In our analysis of the results, we assume the change in reflectivity to be proportional to the change in the electron temperature, $\Delta R \propto \Delta T_e$. This can be justified by the fact that the lattice temperature rise is delayed from that of the electron due to the small electron heat capacity. Thus, at the early stages of laser heating, a small rise in the lattice temperature can be expected and therefore, one can take ΔR to be mainly caused by ΔT_e. In addition, the peak electron temperature rise ΔT_{emax}, predicted from TTM, varies linearly with the fluence which is also the case for the maximum reflectivity change ΔR_{max} as determined experimentally [10]. Finally, since the maximum electron temperature in this experiment is less than 700 K, the measured reflectivity change ΔR can be safely assumed to be proportional to the electron temperature change ΔT_e. This is in line with the findings of Qiu et al. [4] that the aforementioned holds in the regime where $300\ \mathrm{K} < T_e < 700\ \mathrm{K}$, which is also consistent with the results of Juhasz et al. [11].

Fig. 2(a) and (b) show the comparison of our experimental results with the model predictions for 40- and 80-nm thin gold films, respectively. Predictions from the TTM follow the decaying part of the experimental results. However, the TTM is unable to account for the

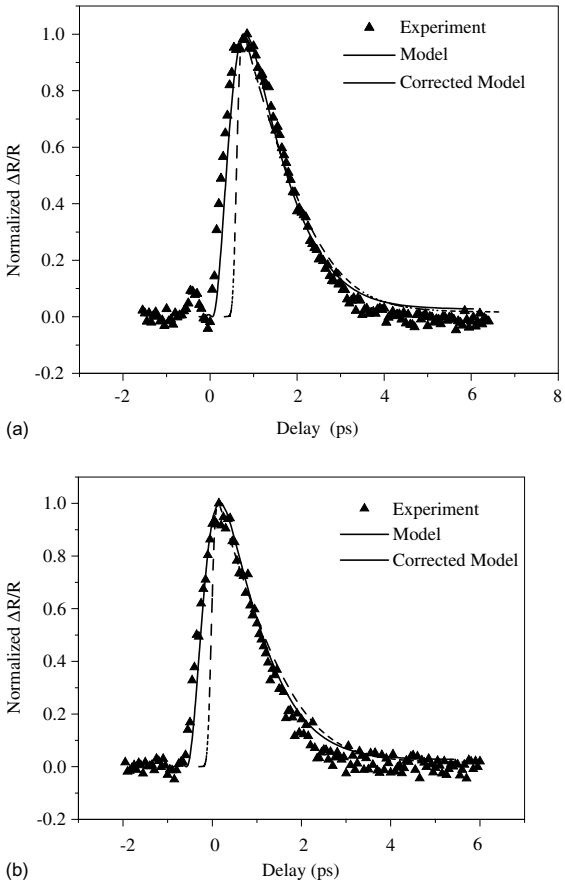

Fig. 2. Comparison between the experimental results, the TTM, and the model taking into effect convolution and thermalization effects for (a) Au 40 nm, and (b) Au 80 nm, laser incident fluence was 2.7 mJ cm^{-2}.

first few hundred femtoseconds of the heating process. This discrepancy will be addressed later in the paper. In the model fit to the experiment, we chose the $t = 0$ ps to correspond to the time with maximum thermomodulation for the experimental data and maximum electron temperature for model calculation. These times are close to each other but not necessarily overlapping due to convolution effects. Convolution effects can cause temporal broadening of the measured signal, especially when the interrogating (probe) pulse is on the same time scale as the physical quantity to be measured, in this case, the thermoreflectivity signal. The decay time of the normalized thermoreflectivity signal at the front surface of Au 40- and 80-nm films irradiated with 280 $\mu J\,cm^{-2}$, $\lambda = 800$ nm, 150 fs (FWHM) pulses, is basically the same for both samples. This is in agreement with the result of Wellerschoff et al. [8] that for samples with thickness $\leqslant 100$ nm electron transport is mostly ballistic. The transient decay time of the experimental thermoreflectivity signal is determined by fitting the decay signal, starting from 90% of the peak down to 1/e of the peak, to an exponential decay function. Using this decay time, we get $G = 2.3 \times 10^{16}\ W\,m^{-3}\,K^{-1}$ for the 40- and the 80-nm samples, consistent with values published in the literature [1]. This G value was used in all our modeling.

The discrepancy between the model prediction and the experiment in the first few hundreds of femtoseconds can be explained by the findings of Fann et al. [12]. Their results clearly indicated the overlap of the time scales for the electron thermalization and the electron–phonon energy transfer. Therefore, the electron temperature could not be well defined, at least for the first few hundred femtoseconds, and hence the TTM is not valid in this time interval. Convolution effects between the pump and probe pulses can also contribute to this discrepancy as explained above. Sun et al. [13] used a system response function that introduced a delayed rise time of the signal due to the build up of the Fermi distribution temperature through energy transfer from the nonthermal distribution by e–e interactions. They convoluted the response function with the measured pump–probe correlation data. Their approach led us to convoluting the system response function, due to convolution and internal thermalization effects, with the model. This is due to the fact that the actual measured data already include effects of convolution whereas, the model does not account either for the convolution effects or the internal thermalization of electrons. The response function we used is of the form:

$$S(t) = u(t)\left[1 - \exp(-t/\tau_R)^2\right] \tag{4}$$

where τ_R accounts for the internal thermalization time which is derived from the experimental data (~500 fs) and is in agreement with the results of Fann et al. [12]. The results of adding this response function are shown in Fig. 2(a) and (b). The model predictions showed good agreement with the experimental results.

Fig. 3(a) shows a comparison between the experimental results for Au 40-nm and Au–V 20/20 nm multilayer film. The choice of sample thickness was made to be able to safely exclude diffusion effects since the laser penetration depth (13 nm) is comparable to the thickness of the top gold layer. The thermoreflectivity signal for the multi-layer film experiences a reduction of ΔR_{max} by around 45% that signifies a reduction in the surface electron temperature. In the case of the multi-layer sample, it is expected that the ballistic electrons reach the back surface of the top gold layer within 20 fs assuming they have a velocity about the Fermi velocity of $10^6\ m\,s^{-1}$. As these ballistic electrons cross over into the vanadium layer they start coupling their energy to the lattice much faster than their counterparts in the top

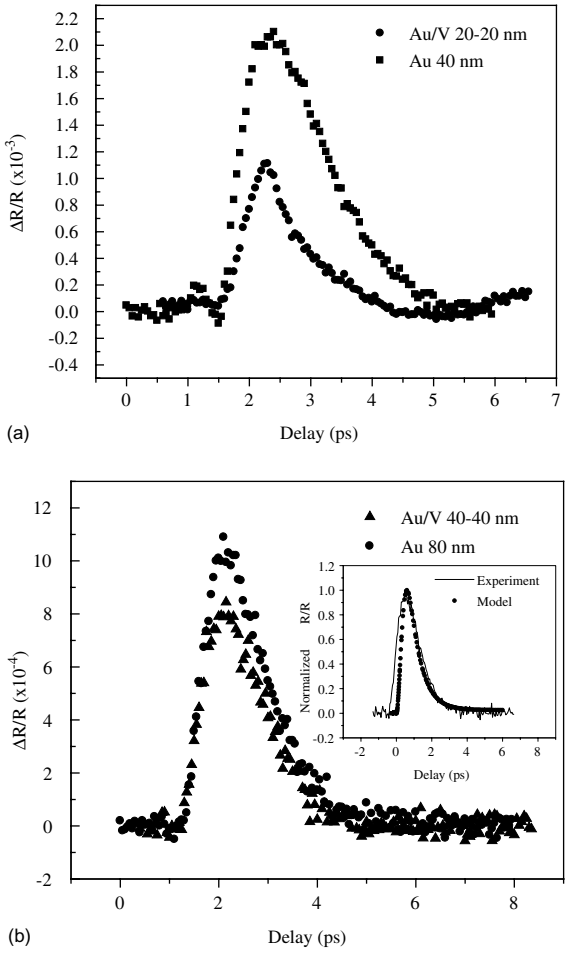

Fig. 3. Comparison between the change in reflectivity for (a) Au 40 nm and Au–V 20–20 nm, and (b) Au 80 nm and Au–V 40–40 nm, laser fluence used was 1.3 $mJ\,cm^{-2}$. The inset in (b) shows a fit of the TTM to the data.

gold layer due to the large e–ph coupling coefficient in vanadium. Thus reducing the surface effective electron temperature of gold.

Energy deposition and transport was also tested in 80-nm single gold layer and gold–vanadium double-layer structure. A reduction of ΔR_{max} by $\sim$22%, as shown in Fig. 3(b), in the thermoreflectivity signal for the multi-layer film signifies a reduction in the surface electron temperature. The inset of Fig. 3(b) shows the model comparison with the experimental results for the 80-nm gold–vanadium double-layer structure. It was suggested that the noisy signal at the early stages of laser heating is due to the interference between the pump and probe laser pulses [4].

In order to extend our investigations into the damage regime, we resorted to our model to determine the damage threshold for both samples. In the model, the electron and heat flux at the gold–vanadium interface are continuous, thus neglects interface resistance. We define the damage threshold as the laser fluence causing the surface lattice temperature to reach the melting point of gold, i.e., $T_l = 1336$ K. According to the model, the fluence needed for the lattice surface temperature to attain the melting point is 0.3 J cm^{-2} for both films. The model reveals a higher peak electron temperature for the single layer gold film, 7645 K, as compared with the multi-layer gold–vanadium film, 7434 K. Fig. 4(a) shows the model predictions, with the ballistic term included, for the lattice temperature at the surface and 1 nm after the interface for the multi-layer sample, using a fluence of 0.25 J cm^{-2}. It is apparent that the padding layer acts as a heat sink for the deposited electron energy in the first stage of heating while the lattice surface temperature is hardly affected. The lattice temperature after the interface reaches around 800 K, while the gold surface lattice temperature is still around 400 K. This substantiates the postulate that the ballistic electrons couple their energy to the lattice of the padding layer. The large G value for V, results in a strong coupling of the electron energy to the lattice generating a strong lattice heating at the interface. The surface temperature decays in $\sim$1 ps. However, since the electron temperature cannot fall below that of the lattice, the lattice temperature gradient established at the interface results in hot electron diffusion from the interface towards the surface. This back electron diffusion raises the temperature of the gold layer as shown in Fig. 4(b).

In the damage experiments, the single layer samples used were gold 50 and 80 nm thickness. The multi-layer structures were gold–vanadium–gold 15–20–45 nm and 16–23–50 nm. This enabled us to test the effect of introducing a padding layer under the top gold layer. The layer of gold in contact with the sapphire was to assure that no stress related effect at sapphire interface is changing the damage threshold between the single layer and multi-layer films. A surface scan of the samples was

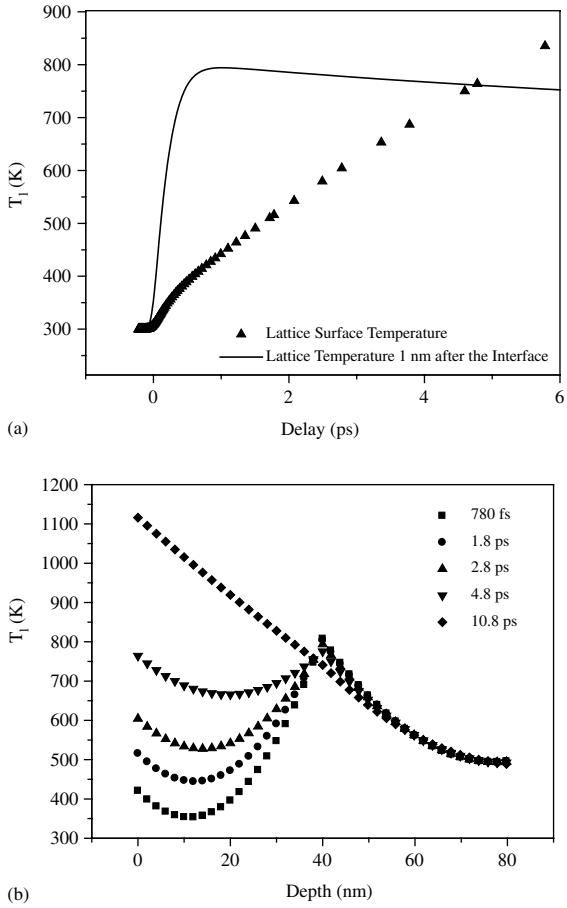

Fig. 4. Predictions of the TTM for (a) the lattice temperature at the surface and 1 nm after the interface, and (b) the depth profile of the lattice temperature, for the Au–V 80-nm film. The laser fluence is 0.25 J cm^{-2}.

done using transmission and reflection measurements to ensure uniformity of the samples' thickness and to obtain a value for the samples' absorption at the incident wavelength. A surface roughness measurement was obtained using atomic force microscopy (AFM). Both single and multi-layer samples had comparable roughness. The onset of damage was detected by optical microscopy. An onset of damage was evident at $\sim$0.3 J cm^{-2} for the single layer, whereas the multi-layer showed an early onset of damage at a relatively close value of $\sim$0.22 J cm^{-2}. The results were generally reproducible on different samples fabricated and tested under the same experimental conditions.

The apparent reduction in the damage threshold for the multi-layer film is not explained by the present TTM model, but could be related to the hot-electron blast proposed by Tzou et al. [5]. The deformation in the film, caused by ultrafast heating, was found to be much more significant in the interface of multi-layer films with dis-

similar electron–phonon coupling. This deformation can cause mechanical damage to the film at a temperature below the melting threshold [5]. Other processes that could affect the damage threshold might be related to the interface quality, which is sensitive to the preparation conditions. We have assumed that electrons pass through the Au–V interface without any reflections, which might not be the case especially for a rough interface. We also note that the determination of the damage threshold by optical microscopy is subject to a relatively large error.

Guo and Taylor, through time-resolved measurement of the dielectric function, have observed ultrafast electronic disorder in femtosecond laser heating of Au [14]. The photon energy of their laser (1.55 eV) was similar to ours, which is lower than the onset of the top of the d-band to Fermi level transition in Au (2.45 eV) [14]. The electronic induced structural phase transition, probed by the sudden dielectric constant change, occurred at the melting threshold. Thus, the assumption that the damage threshold corresponds to the laser fluence causing the surface lattice temperature to reach the melting point of Au is reasonable even though the mechanism of melting under femtosecond excitation is complex. For other metals and for Au heated by different laser photon energy, the assumption that damage corresponds to thermal melting might not be valid.

The obtained damage results do not contradict the thermomodulation results that the padding layer reduces the surface effective electron temperature. The thermomodulation results on Au–V are in agreement with the those previously obtained for Au–Cr [3,4], which investigated the heating regime for 300 K $< T_e <$ 700 K. However, for the higher fluence regime, the V padding layer does not improve the Au surface damage threshold.

5. Conclusions

Femtosecond time-resolved thermoreflectivity ($\Delta R/R$) measurements on polycrystalline single layer gold films and multi-layer Au–V films were conducted. The experimental results are analyzed within the framework of the TTM, which describes the energy relaxation in ultrafast heating. A comparison between the experimental results for Au 40-nm and Au–V 20–20 nm multi-layer film revealed a reduction of the thermoreflectivity signal, ΔR_{max}, for the multi-layer film that signifies a reduction in the surface electron temperature. In the case of the multi-layer sample, it is believed that the ballistic electrons establish an extended energy deposition depth in the gold layer in the first few tens of femtoseconds. Then, as these ballistic electrons cross over into the vanadium layer, they couple their energy to the lattice much faster than their counterparts in the top gold layer due to the large e–ph coupling coefficient in vanadium. This effect helps in reducing the electron surface temperature of gold.

At the high fluence regime, the damage experiments revealed an early onset of surface damage in the case of multi-layer samples as compared to the single layer gold sample. This could be due to heat propagation back from the Au–V interface to the surface and nonthermal damage.

Acknowledgements

HE acknowledges the support of the National Science Foundation under Grant No. DMR-9988669 and the US Department of Energy, Division of Material Sciences, under Grant No. DE-FG02-97ER45625.

References

[1] T.Q. Qiu, C.L. Tien, Short-pulse laser heating on metals, Int. J. Heat Mass Transfer 35 (3) (1992) 719–726.
[2] T.Q. Qiu, C.L. Tien, Size effects on non-equilibrium laser heating of metal films, J. Heat Transfer 115 (1993) 842–849.
[3] T.Q. Qiu, C.L. Tien, Femtosecond laser heating of multi-layer metals-I. Analysis, Int. J. Heat Mass Transfer 37 (1994) 2789–2797.
[4] T.Q. Qiu, T. Juhasz, C. Suarez, W.E. Bron, C.L. Tien, Femtosecond laser heating of multi-layer metals-II. Experiments, Int. J. Heat Mass Transfer 37 (1994) 2799–2808.
[5] D.Y. Tzou, J.K. Chen, J.E. Beraun, Hot-electron blast induced by ultrashort-pulsed lasers in layered media, Int. J. Heat Mass Transfer 45 (2002) 3369–3382.
[6] S.I. Anisimov, B.L. Kapelovich, T.L. Perel'man, Electron emission from metal surfaces exposed to ultra-short laser pulses, Sov. Phys. JETP 39 (1974) 375–377.
[7] D.E. Gray (Ed.), American Institute of Physics Handbook, 3rd ed., McGraw-Hill, New York, 1972.
[8] S.-S. Wellerschoff, J. Hohlfeld, J. Güdde, E. Matthias, The role of electron–phonon coupling in femtosecond laser damage of metals, Appl. Phys. A 69 (1999) S99–S107.
[9] J. Hohlfeld, S.-S. Wellerschoff, J. Güdde, U. Conrad, V. Jähnke, E. Matthias, Electron and lattice dynamics following optical excitation of metals, Chem. Phys. 251 (2000) 237–258.
[10] H.E. Elsayed-Ali, T. Juhasz, Femtosecond time-resolved thermomodulation of thin gold films with different crystal structures, Phys. Rev. B 47 (1993) 13599–13610.
[11] T. Juhasz, H.E. Elsayed-Ali, X.H. Hu, W.E. Bron, Time-resolved thermoreflectivity of thin gold films and its dependence on the ambient temperature, Phys. Rev. B 45 (1992) 13819–13822.
[12] W.S. Fann, R. Storz, H.W.K. Tom, Electron thermalization in gold, Phys. Rev. B 46 (20) (1992) 13592–13595.

[13] C.K. Sun, F. Vallee, L. Acioli, E.P. Ippen, J. Fujimoto, Femtosecond Investigation of electron thermalization in gold, Phys. Rev. B 48 (1993) 12365–12368.

[14] C. Guo, A.J. Taylor, Ultrafast electronic disorder in heat-induced structural deformation and phase transition in metals, Phys. Rev. B 62 (2000) 5382–5386.